An Experimental Study on the Pumping Performance of Molecular Drag Pumps

Myoung-Keun Kwon
School of Mechanical Engineering, Sungkyunkwan University, 300 Chunchun-dong, Jangan-ku, Suwon 440-746, Korea
Young-Kyu Hwang*
School of Mechanical Engineering, Sungkyunkwan University, 300 Chunchun-dong, Jangan-ku, Suwon 440-746, Korea

The pumping performance of molecular drag pumps (MDP) has been investigated experimentally. The experimented MDPs are a disk-type drag pump (DTDP), helical-type drag pump (HTDP) and compound drag pump (CDP), respectively. In the case of the DTDP, spiral channels of a rotor are cut on both upper surface and lower surface of a rotating disk, and the corresponding stator is a planar disk. In the case of the HTDP, the rotor has six rectangular grooves. The CDP consists with the DTDP, at lower part, and with the HTDP, at upper part. The experiments are performed in the outlet pressure range of 0.2~533 Pa. The inlet pressure and compression ratio are measured under the various conditions of outlet pressure and throughputs, and nitrogen is used for the test gas. At the outlet pressure of 0.2 Pa, the ultimate pressure has been reached to 1.0×10^{-2} Pa for the HTDP, 1.3×10^{-4} Pa for the DTDP, and 3.6×10^{-5} Pa for the CDP. The maximum compression ratio of the CDP is much higher than those of the DTDP or HTDP. Consequently, the ultimate pressure of the CDP is the lowest one.

Key Words : Molecular Drag Pump, Ultimate Pressure, Compression Ratio, Pumping Speed

1. Introduction

With the active development of semiconductor fabrication technology, dilute gas flow phenomena are attracting attention recently. The turbo-type high vacuum pump is a very important subsystem of semiconductor equipment, and it is widely used in etching, low pressure chemical vapor deposition (CVD), metalorganic CVD, ion implantation, and sputtering processes. The main disadvantage of the traditional turbomolecular pump (TMP) is the low pumping efficiency for the inlet pressure over 10^{-5} Pa, where most of the low pressure processing of semiconductor manufacturing is performed. In the pressure over 10^{-5} Pa, a molecular drag pump (MDP) is added between a TMP and foreline mechanical pump.

MDPs have been widely used in high density plasma and etching processes because of their higher discharge pressure and larger throughput. The semiconductor industry is getting into an era by using 300 mm wafers. In the near future, the size of wafer is expected to be magnified to 450 mm, more than size 300 mm of wafer. Therefore, an efficient MDP is rapidly needed to provide an ultra-clean environment and productivity. MDPs are widely used, in combination with a turbo-molecular pump, in order to improve the pumping performance of it (Hablanian, 1990 ; 1994). The MDP may be of the helical-type (Holweck) or

* Corresponding Author,
E-mail : ykhwang@skku.edu
TEL : +82-31-290-7437; **FAX** : +82-31-290-5889
School of Mechanical Engineering, Sungkyunkwan University, 300 Chunchun-dong, Jangan-ku, Suwon 440-746, Korea. (Manuscript **Received** September 9, 2005; **Revised** June 13, 2006)

disk-type (Siegbahn) designs.

Nanbu et al.(1991) numerically studied the molecular transition and slip flows in pumping channels of a HTDP. They found that most of the pressure rise occurs near the outlet of the channel. Shi et al.(1993) theoretically investigated the influence of geometrical parameters of a spiral channel on performance. According to their studies, the performance is strongly dependent on the rotational speed and geometrical parameters.

In the molecular drag pump, such as the cylindrical-type (helical-type) molecular drag pump and the Siegbahn (disk-type) molecular drag pump, the length of pumping channel is long but that of leakage is relatively short. Hence, narrow leakage channel, i.e., the gaps between rotating and stationary parts, have to be adopted to obtain a higher compression ratio (Chu, 1987).

Recently, Hwang and Heo (2000; 2001) numerically studied the molecular transition and slip flows by using both the direct simulation Monte Carlo method (DSMC) and the Navier-Stokes equations with slip boundary conditions in a HTDP and DTDP. Also, Hwang and Kwon (2004) numerically studied the effect of the vertical clearance between a rotor and stator on pumping performance of a DTDP.

The present experimental study is performed to investigate the pumping characteristics of three kinds of MDPs in the molecular transition flow region. Experimented pumps are a disk-type molecular drag pump (DTDP), helical-type molecular drag pump (HTDP) and compound molecular drag pump (CDP), respectively. The DTDP consists with three rotors and four stators. The HTDP consists of a helical rotor which has six grooves. The CDP is constituted by the combination of the above three-stage DTDP, at lower part, and the HTDP at upper part. We have measured the inlet pressure P_1, compression ratio K and pumping speed S_P for each MDP under various conditions of outlet pressure P_2 and throughput Q, respectively. The pumping characteristics of each MDP will be compared with others. It will be seen that the CDP shows the best pumping performance owing to the special role of the combined rotor.

2. Experimental Devices and Method

2.1 Experimental apparatus

The layout of the experimental setup is shown in Fig. 1. The experimental apparatus are composed of a MDP, vacuum gauge sensors, fore-line backing pump and mass flow-meter control (MFC) for flow measurement. The test pump (MDP) is connected to a two-stage oil rotary vane pump (970 l/min, WooSung Vacuum Co. Ltd.). The pressure in the high-vacuum side is measured with a Pirani guage ($10^{-1}\sim10^{2}$ Pa, ULVAC Co. Ltd.) and ionization gauge ($10^{-7}\sim10^{-1}$ Pa, Varian Co. Ltd), and the pressure in the fore-vacuum side is measured with a Pirani gauge.

A three-stage DTDP and a single-stage HTDP are shown in Figs. 2(a) and (b), respectively. Also, a CDP is shown in Fig. 2(c). The DTDP consists with three spirally channeled rotors and planar four stators. Namely, spiral channels of the DTDP are cut on both the upper and lower surfaces of rotors, but the stationary stators are planar. Rotors are made of a high-strength aluminum alloy.

As seen in Fig. 3(a), each rotor of the DTDP has 10 Archimedes' spiral channels, and the channel depth d_D is dependent on the number of stage. Namely, the channel depth corresponding to the first stage is chosen as a relatively large value d_D=5 mm in an attempt to intake a large flow rate, while the ones corresponding to the second

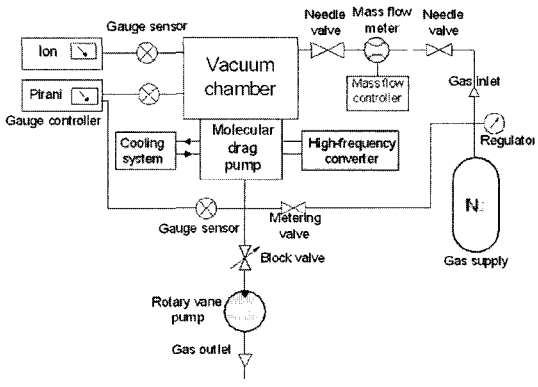

Fig. 1 Schematic diagram of experimental setup

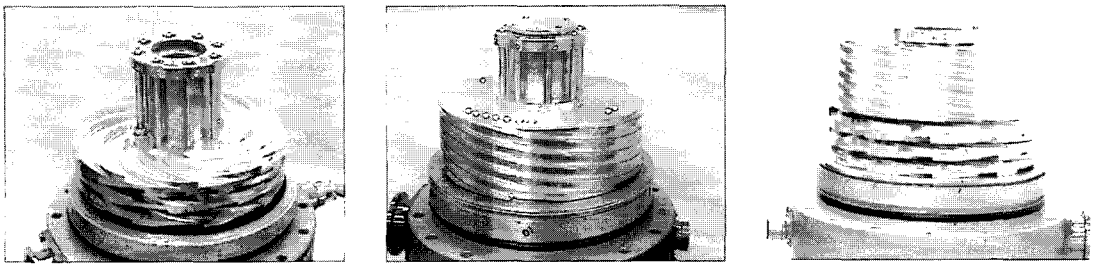

(a) (b) (c)

Fig. 2 Molecular drag pumps: (a) three-stage DTDP, (b) HTDP and (c) CDP

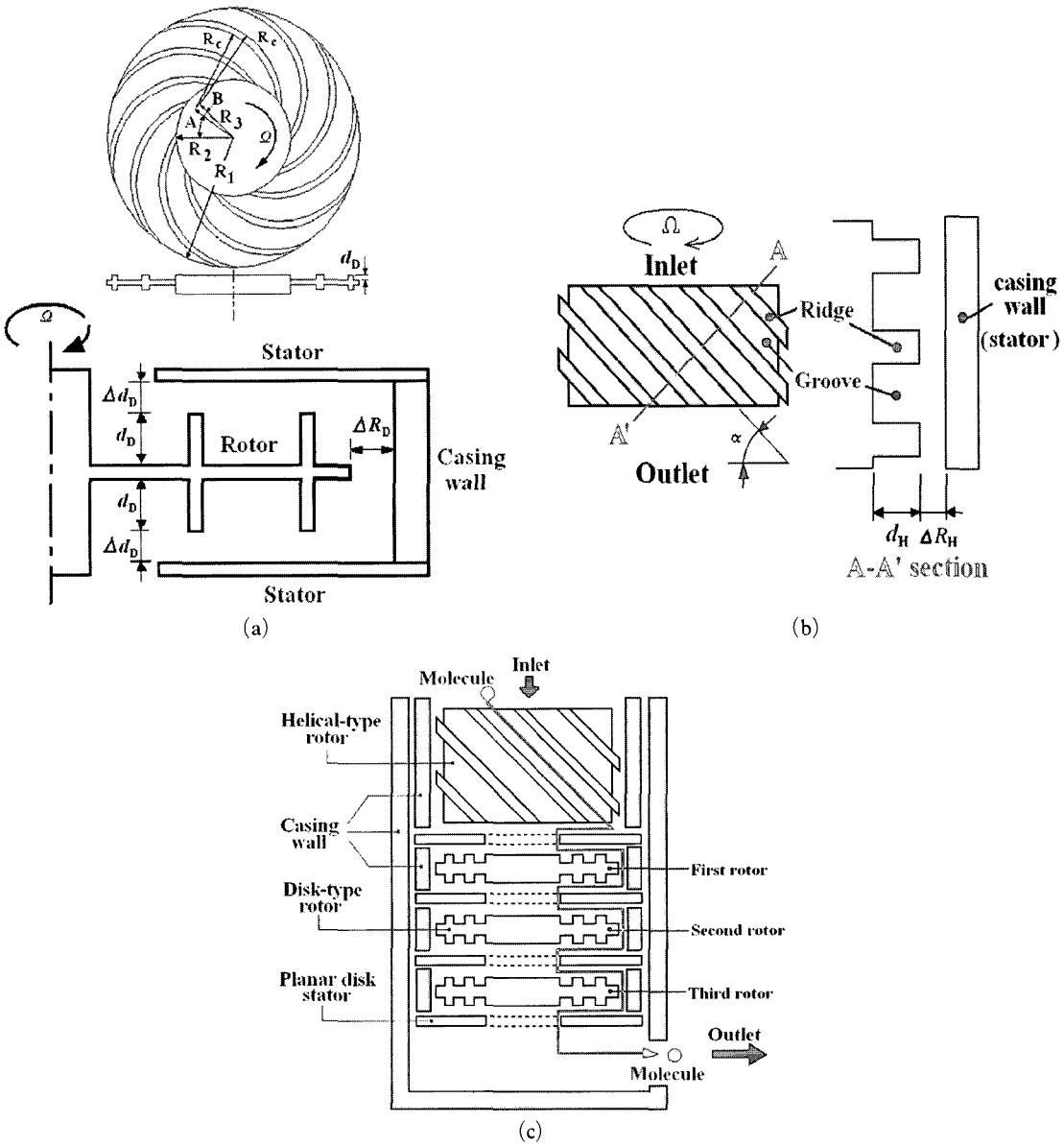

Fig. 3 Geometry of molecular drag pumps: (a) DTDP rotor, (b) HTDP rotor and (c) cross-section of CDP

Table 1 Dimensions of DTDP rotors

Geometry parameters	Symbols	Dimensions
outer radius	R_1	86 mm
inner radius	R_2	39 mm
depth of channel (first stage)	d_D	5 mm
depth of channel (second & third stage)		3 mm
vertical clearance between rotor and stator	Δd_D	0.5 mm
radial clearance between rotor and casing wall	ΔR_D	1 mm
angle of channel inlet	A	36°
angle of channel wall	B	8°
radius of channel	R_C	56 mm
radius of channel center	R_3	32 mm
length of channel	L_D	218 mm
number of grooves	N_D	10

Table 2 Dimensions of HTDP rotor

Geometry parameters	Symbols	Dimensions
diameter of rotor	D_H	169 mm
height of rotor	H	54.5 mm
length of channel	L_H	465 mm
depth of channel	d_H	5 mm
radial clearance between rotor and casing wall	ΔR_H	1 mm
helix angle	α	15°
number of grooves	N_H	6

stage and the third stage are kept as rather small value d_D=3 mm to achieve high compression of a gas, associated with small back flow rates through clearances (see Fig. 3(a), (c) and Table 1). The various channel depth at each rotor may be adopted to increase the mass flow rate and compression ratio. The vertical clearance Δd_D between the rotors and the stators is 0.5 mm, and the radial clearance ΔR_D between the rotors and casing wall is 1 mm, respectively. The detailed geometric dimensions of rotors are shown in Table 1.

As seen from the configuration of the HTDP in Figs. 2(b) and 3(c), the cylindrical rotor of the HTDP has six rectangular grooves. The radial clearance ΔR_H between the helical rotor and casing wall is 1 mm. The profiles of blades, such as the helix angle α, channel depth d_H and channel shapes, are carefully designed to enhance the pumping speed. The detailed geometric parameters of the rotor are shown in Fig. 3(b) and Table 2. The gas entering the rotor is transmitted into the helical grooves of the rotor from top to bottom.

Figure 2(c) show the CDP which is constituted by the three-stage DTDP, at lower part, and the HTDP, at upper part. The design and the assembly procedure of the HTDP part are easier than those of the DTDP part. The helical rotor shape of the CDP is suitable to intake large throughput due to its large cross-sectional area of gas flow. Moreover, it is clear that the relatively longer length of rotating channels will provide better pumping performance of high compression and large pumping speed. Thus, the long pumping channels of three-stage DTDP portion in the CDP will enhance throughput such as a mechanical booster.

Several studies on the rotor shapes of MDPs associated with pumping performance were performed numerically and experimentally by Hwang and Heo (2000; 2001); Hwang and Kwon (2004). They rather completely investigated the effect of the geometric parameters of MDPs on the pumping characteristics. We do not mention in detail concerning the design of geometric parameters.

2.2 Experimental method

Experiments are performed by varying the outlet pressure P_2 in the range of $0.2 \leq P_2 \leq 533$ Pa. The rotational speed of rotors is 24,000 rpm, and it is controlled by a frequency converter. The motor casing of pump is cooled by water at 22±3℃ to prevent overheating easily because it is to rotate with high speed. Nitrogen gas (N_2), which is supplied through a MFC from a regulated high-pressure cylindrical tank, is used for the test gas to measure pumping flow rates.

The vacuum chamber is connected to a MDP system and fore-pump (oil rotary vane pump, 970 l/min, Woo Sung Vacuum Co. Ltd.). That is evacuated sufficiently before experiment. The test pump has to be maintained less than 1 Pa and

cooling systems are operated. The flow rate of the gas admitted into the suction side is measured by a MFC. The control of flow is performed by a MFC and variable leak valve.

3. Results and Discussion

The experiments for pumping performance are carried out for the three kind of MDPs in the outlet pressure range of $0.2 \leq P_2 \leq 533$ Pa. Consequently, their pumping characteristics are obtained with respect to the pumping speed S_P and the maximum compression ratio K_{max}. The experiments are performed three times to ensure stable flow and to obtain converged data. These results under the condition of zero throughput are shown in Figs. 4-5. In particular, the results at various throughputs are shown in Figs. 6-11.

3.1 Ultimate pressure and maximum compression ratio

The relations between the inlet pressure P_1 and the outlet pressure P_2 at zero throughput ($Q=0$ sccm), corresponding to the three MDPs, are shown in Fig. 4. The symbols of solid rectangular denote the measured values of P_1 corresponding to the CDP. Also, the symbols of solid circle and those of solid triangle denote values of P_1 corresponding to the DTDP and to the HTDP, respectively. In both cases of the DTDP and CDP, the value of P_1 is decreased precipitously when P_2 is changed from 533 to 267 Pa, but P_1 is decreased gradually for $P_2 \leq 133$ Pa. In the case of the HTDP, P_1 decreases almost linearly as P_2 decreases in the range $0.2 \leq P_2 \leq 533$ Pa. At $P_2=0.2$ Pa, the ultimate pressure has been reached to 1.0×10^{-2} Pa for the HTDP, 1.3×10^{-4} Pa for the DTDP, and 3.6×10^{-5} Pa for the CDP. The inlet pressure for the CDP is the lowest one, while that for the HTDP is the highest one in the same range of P_2. The ultimate pressure of a vacuum pump is the extreme value towards which the pressure in a test dome (or chamber) tends asymptotically, without introduction of gas and with the pump operating normally.

From the experimental results, the relations between K_{max} and P_2 for the three MDPs are shown in Fig. 5. The definition of K_{max} is the ratio of P_2 to P_1 at zero throughput ($Q=0$ sccm). The value of K_{max} is about 10^2 at $P_2=4$ Pa for the HTDP, and 5×10^3 at $P_2 \approx 1.3$ Pa for the DTDP, and 10^5 at $P_2 \approx 10.7$ Pa for the CDP, respectively. In both cases of the DTDP and the CDP, K_{max} is increased steeply in the range $267 \leq P_2 \leq 533$ Pa. But, the values of K_{max} are nearly constant in the range $1.3 \leq P_2 \leq 80$ Pa. In this range, the similar pattern is observed for the case of the HTDP. For $P_2 \leq$ 100 Pa, the CDP produce higher K_{max} than do the DTDP or the HTDP. This is because the longer rotating pumping channels of the CDP have a more significant effect on the maximum compression ratio than do the DTDP (Heo and

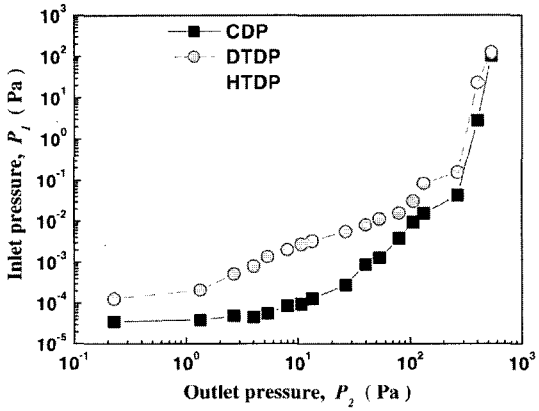

Fig. 4 Ultimate pressure P_1 vs. outlet pressure P_2 for three MDPs at zero throughput

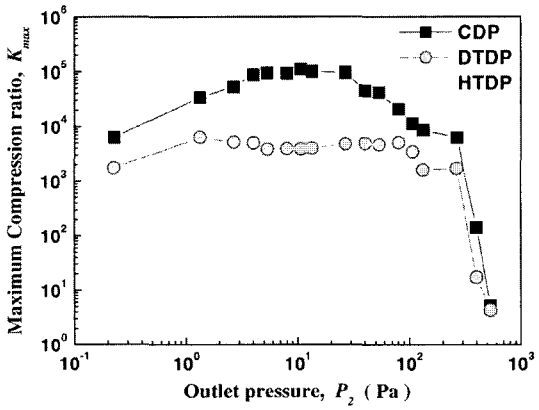

Fig. 5 Maximum compression ratio K_{max} vs. outlet pressure P_2 at zero throughput

Hwang, 2002) or the HTDP. It will be discussed in detail later.

The experimental study on the DTDP by Kwon et al.(2003) for the effect of the number of rotor stages on the pumping performance indicates that the compression ratio and pumping speed were found to be enhanced according to the increase in the total length of rotating channels or the number of rotor stages.

The pumping efficiency w of MDPs can be obtained by

$$w=\frac{N_{12}-N_{21}}{N_i} \tag{1}$$

in which $N_{12}(N_{21})$ is the number of molecules to be transmitted through the channel from the inlet (or outlet) to the outlet (or inlet), and N_i is the number of molecules coming from the inlet during sampling time. The pumping speed S_P and compression ratio K are proportional to the pumping efficiency w (Heo and Hwang, 2002). Namely, if N_{21} becomes smaller, then w, S_P, and K become larger. It means that the pumping speed and compression ratio are enhanced significantly by reducing the back streaming flow rates.

3.2 Pumping performance of mass flow rate

The effect of the outlet pressure on the inlet pressure is shown in Figs. 6-7 at Q=66 and 200 sccm, respectively. The inlet pressure becomes higher as the mass flow rate increases. Also, it depends on the outlet pressure. Namely, the values of P_1 for three MDPs are nearly constant in the outlet pressure range of $P_2 \leq 133$ Pa, but their slopes are very steep in the range of $133 \leq P_2 \leq 533$ (see Fig. 6). In both cases of the CDP and DTDP, P_1 is decreased abruptly when P_2 is changed from 533 to 133 Pa. On the other hand, it is nearly constant in the range $27 \leq P_2 \leq 133$ Pa. In the case of the HTDP, P_1 is decreased linearly in the range $80 \leq P_2 \leq 533$ Pa. Because the pumping performance of pumps reach to limits of the pump's work when the mass flow rate increases gradually more. The experimental results in Fig. 7 show the similar pattern observed in Fig. 6.

Figures 8 and 9 show the relation between P_2 and compression ratio K at given Q=66 and 200 sccm, respectively. The definition of compression ratio K is the ratio of outlet pressure P_2 to inlet pressure P_1, for a given gas. At Q=66 sccm, the highest value of K for the CDP is about 60 at P_2=133 Pa ; 25 for the DTDP at P_2=133 Pa ; 10 for the HTDP at P_2=80 Pa. The compression ratio is deteriorated significantly due to the leakage of gas flow as P_2 is decreased (see Fig. 8). At the fixed value of Q=200 sccm, the highest value of K for the HTDP is about 5 at P_2=107 Pa ; 10 for the DTDP at P_2=133 Pa ; 25 for the CDP at P_2=267 Pa (see Fig. 9). It means that the DTDP compresses the gas more effectively than dose the HTDP. This is because of its relatively long length of rotating pumping channels with the small clearance between the rotor and stator (Δd_D=0.5 mm).

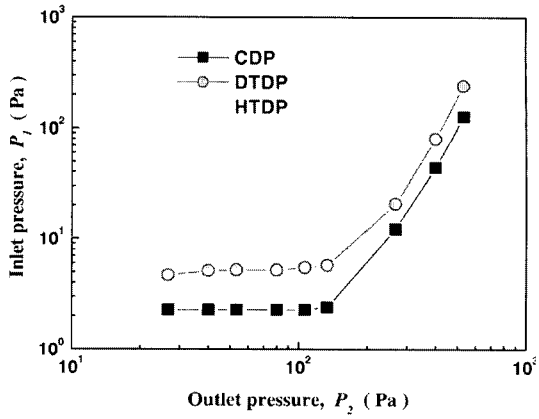

Fig. 6 Inlet pressure P_1 vs. outlet pressure P_2 at Q=66 SCCM

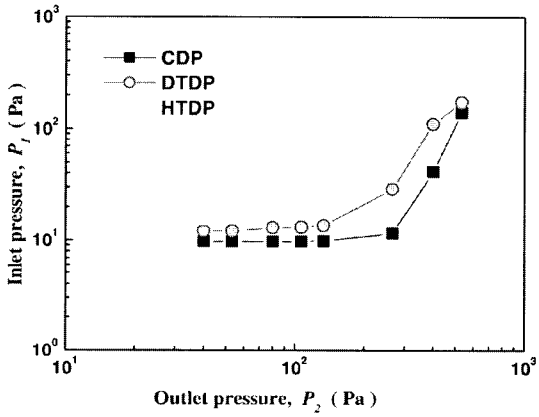

Fig. 7 Inlet pressure P_1 vs. outlet pressure P_2 at Q=200 SCCM

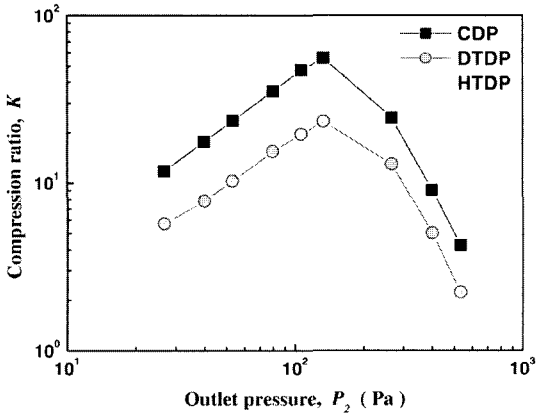

Fig. 8 Compression ratio K vs. outlet pressure P_2 at Q=66 SCCM

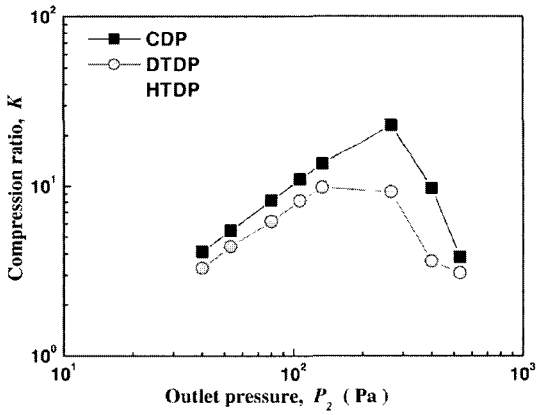

Fig. 9 Compression ratio K vs. outlet pressure P_2 at Q=200 SCCM

It is noted that the cross sectional flow area of the HTDP rotor is relatively larger than that of the DTDP rotor, since the channel depth d_H of the HTDP rotor is deeper than that of the DTDP rotor. Also, the total pumping channel length of the HTDP (L_H=465 mm) is shorter than that of the DTDP (L_D=218 mm/stage×3 stages=654 mm).

However, the pumping performance of the CDP is much better than those of the DTDP or the HTDP. Namely, its total pumping channel length is increased by the combination of the HTDP and DTDP. This causes to enhance the compression ratio and the pumping speed significantly. The HTDP rotor, at the upper part of the CDP, plays a role of mechanical booster for high flow rates.

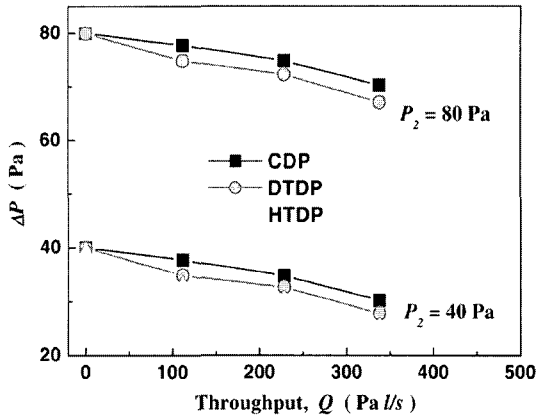

Fig. 10 Pressure difference ΔP vs. throughput Q at P_2=80 and 40 Pa

The pressure difference $\Delta P(=P_2-P_1)$ between the inlet pressure and the outlet pressure is given in Fig. 10 as a function of the throughput at P_2= 40 and 80 Pa. The throughput Q increases as ΔP decreases. At P_2=40 Pa, the curves of ΔP corresponding to the three MDPs show that their slopes with respect to Q are almost same. But, at P_2=80 Pa, the slope of ΔP corresponding to the HTDP is more precipitous than those corresponding to the DTDP or the CDP. It is due to the effect of back flow of gas molecules on the pressure field because the pumping channel of the HTDP is smoothly slope, and the channel structure of the radial clearance ΔR_H is not rectangularly changed for all pumping channel of the HTDP.

3.3 Pumping speed

The vacuum pumps used in a vacuum system remove (evacuate) gas from the system. The rate at which the gas is removed is measured by the pumping speed S_p. The value of S_p is defined as the volume of gas per unit of time dV/dt which the pumping device removes from the system at the pressure existing at the inlet to the pump (Hablanian, 1990; 1994). The throughput Q is defined as the product of the pumping speed and the inlet pressure, i.e.

$$Q=P_1S_p=P_1(dV/dt) \tag{2}$$

By analogy with the expression Eq. (1), the pumping speed S_p(l/s) at the point of the vacuum system is

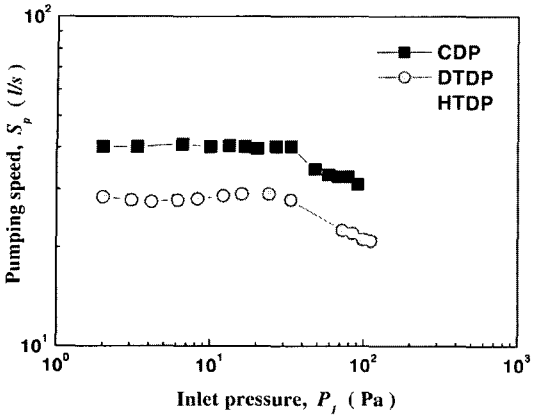

Fig. 11 Pumping speed S_P vs. inlet pressure P_1

$$S_P=\frac{Q}{P_1} \tag{3}$$

in which Q(Pa·l/s) is the throughput in the system, and P_1 is the inlet pressure at the point at which the pumping speed is defined.

The pumping speed of the MDPs is shown in Fig. 11 by using a flow-meter method. The horizontal axis is the inlet pressure P_1 of the pumps, the vertical axis is the pumping speed S_P. In the molecular flow regime, the pumping speed has been reached to 40 l/s for the CDP, 30 l/s for the DTDP, and 20 l/s for the HTDP. In both cases of the CDP and the DTDP, S_P gradually increases as P_1 decreases for $33 \leq P_1 \leq 100$ Pa, and it is nearly constant for of $P_2 \leq 33$ Pa. This is a typical feature of pumping characteristic of common MDPs (Hablanian, 1990 ; 1994). The pumping speed for the HTDP alone is the poorest one due to the shortest length of rotating pumping channels. But, the large cross sectional flow area of the HTDP rotor, at the upper part of the CDP, is suitable for the large pumping speed. Moreover, the long length of rotating pumping channels of CDP, by the combination of the HTDP and DTDP, is necessary for the large pumping speed.

4. Conclusions

The objective of the study was experimentally to analyze pumping characteristics of a composite molecular drag pump. Experiments of pumping performance have been carried out for the HTDP, DTDP, and CDP, respectively. From these experimental results, we have obtained the ultimate pressure, maximum compression ratio, and pumping speed under the various combined conditions of throughput and outlet pressure.

According to the increase in the mass flow rate for the three MDPs, in general, the resulting compression ratio is decreased, while the respective inlet pressure is increased. In the case of zero throughput, the DTDP produce more extreme values of the ultimate vacuum and maximum compression ratio than dose the HTDP. But, the compression ratio of the CDP is much higher than those of the DTDP or HTDP. Thus, the inlet pressure of the CDP is much lower than those of the DTDP or HTDP. Consequently, it is found that the pumping performance of the CDP is the best one associated with the highest compression ratio, lowest inlet pressure, and largest pumping speed, compared to the single-type MDPs (i.e., DTDP and HTDP). This is because not only its relatively larger cross-sectional flow area but also longer pumping channels by the combination of HTDP and DTDP rotors significantly effect on the performance.

In the molecular drag pump, the length of pumping channel is long but that of leakage is relatively short. Hence, it is recommended that the clearances between rotating and stationary parts should be small to achieve a higher compression ratio.

Acknowledgements

This work was supported by Korea Research Foundation Grant funded by Korean Government (MOEHRD) [KRF-2005-202-D00074] and financial aid also from the Korea Ministry of Education through the Brain Korea 21 project is gratefully acknowledged.

References

Chu, J. G., 1987, "A New Hybrid Molecular pump with Large Throughput," *J. Vac. Sci. Technol. A*, Vol. 6, No. 3, pp. 1202~1204.

Hablanian, M. H., 1990, *High-Vacuum Tech-*

nology (*A Practical Guide*), Marcel Dekker, Inc.

Hablanian, M. H., 1994, *In Vacuum Science and Technology : Pioneers of 20th Century*, edited by P. A. Redhead (AIP, New York), pp. 126~132.

Heo, J. S. and Hwang, Y. K., 2000, "Molecular Transition and Slip Flows in the Pumping Channels of Drag Pumps," *J. Vac. Sci. Technol. A*, Vol. 18, No. 3, pp. 1025~1034.

Heo, J. S. and Hwang, Y. K., 2002, "Direct Simulation of Rarefied Gas Flows in Rotating Spiral Channels," *J. Vac. Sci. Technol. A*, Vol. 20, No. 3, pp. 906~910.

Hwang, Y. K. and Heo, J. S., 2001, "Three-dimensional Rarefied Flows in Rotating Helical Channels," *J. Vac. Sci. Technol. A*, Vol. 19, No. 2, pp. 662~672.

Kwon, M. K. and Hwang, Y. K., 2004, "A Study on the Pumping Performance of the Disk-type Drag Pumps for Spiral Channel in Rarefied Gas Flow," *Vacuum*, Vol. 76, No. 1, pp. 63~71.

Kwon, M. K., Heo, J. S. and Hwang, Y. K., 2003, "An Experimental Study on the Pumping Performance of the Multi-stage Disk-type Drag Pump," *Journal of the Korean Vacuum Society*, Vol. 12, No. 2, pp. 79~85.

Nanbu, K., Kubota, H., Igarashi, S., Urano, C. and Enosawa, H., 1991, "Performance of Spiral Grooves on a Rotor of Turbomolecular Pump," *Trans. JSME*, Vol. 57, No. 533, pp. 172~177.

Shi, L., Wang, X. Z., Zhu, Y. and Pang, S. J., 1993, "Design of Disk Molecular Pumps for Hybrid Molecular Pumps," *J. Vac. Sci. Technol. A*, Vol. 11, No. 2, pp. 426~431.

Shi, L., Zhu, Y., Wang, X. Z. and Pang, S. J., 1993, "Influence of Clearance on the Pumping Performance of a Molecular Drag Pump," *J. Vac. Sci. Technol. A*, Vol. 11, No. 3, pp. 704~710.